ACS APPLIED ELECTRONIC MATERIALS

Open Access
This article is licensed under CC-BY-NC-ND 4.0

pubs.acs.org/acsaelm
Article

Direct Physical Vapor Deposition of Liquid Metal on Treated Metal Surface

Ryosuke Matsuda, Yuji Isano, Koki Onishi, Hiroki Ota,* and Fumihiro Inoue*

Cite This: https://doi.org/10.1021/acsaelm.4c02096

Read Online

ACCESS | Metrics & More | Article Recommendations | Supporting Information

ABSTRACT: Liquid metal has garnered significant interest as a potential stretchable wiring material for next-generation stretchable electronics. The operation of substrates within these electronics necessitates adherence to three primary criteria for the wiring of electronic substrates to facilitate the integration of stretchable circuits in society. First, the wiring's top surface must remain exposed to allow for the straightforward attachment of electronic components following the wiring fabrication. Second, the design of the wiring pattern should not be subject to significant constraints. Third, the substrate's top surface needs to be clean and devoid of excess conductive material to mitigate the risk of unintended short-circuits. Previous studies have not introduced a liquid metal patterning method that meets all of these criteria. Physical vapor deposition (PVD) is commonly employed for depositing hard metals on nonstretchable substrates such as silicon and glass. However, when subjected to direct PVD, liquid metal forms independent nanoparticles, losing conductivity due to its exceptionally high surface tension and the presence of surface oxide films. Consequently, the direct deposition of liquid metals without subsequent physical stimulation, such as the application of pressure, has been deemed challenging. In our study, we enhanced the substrate surface's wettability by treating it with copper chloride, thereby facilitating the direct deposition of liquid metals onto the substrate surface. The oxide film on the liquid metal's surface is disrupted upon contact with the copper chloride-treated substrate, enabling the nanoparticles to coalesce and establish electrical connectivity, thereby preserving conductivity even when stretched. The resultant stretchable wiring exhibited a fine line width of approximately 50 μm and a thin film thickness of approximately 1 μm, ensuring a robust bond with the substrate surface. Consequently, this wiring technique supports diverse patterning designs when combined with processing methods such as photolithography.

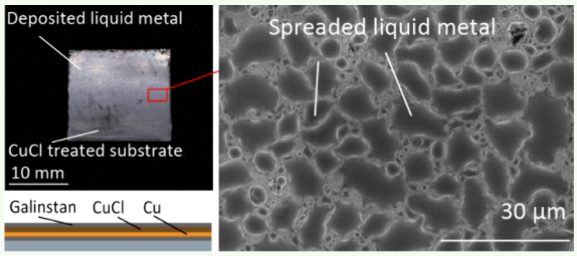

KEYWORDS: *liquid metal, vapor deposition, surface treatment, microparticle, stretchable device*

Downloaded via YOKOHAMA NATL UNIV on April 15, 2025 at 13:15:51 (UTC).
See https://pubs.acs.org/sharingguidelines for options on how to legitimately share published articles.

INTRODUCTION

The surge in research focused on stretchable electronic devices is largely fueled by the proliferation of wearable devices,[1,2] electronic skin,[3−7] and soft robotics.[8−11] Traditional electronic devices and wiring materials, primarily crafted from solid metals such as copper on rigid substrates such as silicon, face a significant drawback: susceptibility to breakage under strain. To mitigate this problem, gallium-based liquid metal alloys are increasingly utilized as stretchable conductive materials.[12−16] These liquid metals, due to their inherent elasticity and higher conductivity compared with other stretchable materials such as conductive polymer composites, present a compelling alternative for crafting highly stretchable substrates and electronic systems.

The application of liquid metal as electronic wiring necessitates its patterning in diverse shapes on the substrate and direct connection to electronic elements. Various methodologies have been explored for this purpose, including the channel method,[17−19] stencil printing method,[20−23] dispensing method,[24,25] laser sintering method,[26,27] and imprinting method.[28] However, these approaches often encounter issues such as limitations in pattern shapes and line widths, the requirement for maintaining substrate surface cleanliness, and challenges in opening the top surface of the wiring.

Other methods have been proposed for patterning liquid metal on substrate surfaces by enhancing wetting through changes in the physical properties of the surface, such as optimizing roughness and creating micropillars.[29−31] In these studies, a physical structure is preconstructed on the substrate surface, which prevents the liquid metal from forming particulates, thus achieving uniform wetting and spreading. However, as these methods form microstructures on the substrate, the patterning accuracy of the liquid metal depends on the structure. While these methods are effective for forming

Received: November 22, 2024
Revised: March 21, 2025
Accepted: March 21, 2025

ACS Publications
© XXXX The Authors. Published by American Chemical Society

https://doi.org/10.1021/acsaelm.4c02096
ACS Appl. Electron. Mater. XXXX, XXX, XXX−XXX

stable liquid metal films over large areas, they face challenges in patterning fine lines on the order of tens of micrometers.

Additionally, studies have focused on selectively improving the wettability of liquid metal and substrates by prepatterning gold[32,33] or tin[34] These methods exploit the good wettability between solid metal and liquid metal by patterning the solid metal at the location where the liquid metal film is to be applied. The liquid metal is then directly applied from the top surface, with excess material removed using a roller or squeegee. This approach offers higher patterning accuracy than the microstructure method described above. However, it requires physical rubbing of the substrate surface to remove excess liquid metal, which may damage the substrate. Thus, a need for a wiring processing technique that supports an open top surface, allows for varied patterning shapes, and maintains clean substrate surfaces is evident.

To meet the requirements for fabricating wiring on hard substrates, the physical vapor deposition (PVD) method has emerged as a technique due to its ability to precisely control film thickness and create diverse patterning shapes when integrated with lithography technology. PVD is widely used in batteries,[35−37] semiconductor electronics[38,39] and sensors,[40] and it is believed that the technology for creating liquid metal patterns via vapor deposition will be key in the future. A significant advantage of this patterning method is its elimination of the need to seal the wiring's top surface, leveraging the strong adhesion between the metal and the substrate surface.[41] This characteristic is particularly beneficial for the subsequent application of electronic elements onto the patterned wiring. In a previous study, a method for producing liquid thin films through vapor deposition of single gallium metal was proposed.[42] However, metallic gallium has a melting point of approximately 30 °C, rendering it solid at standard room temperature and posing challenges for temperature control in general mechanical applications. To address this issue, alloying gallium with other metals to lower the melting point has been suggested. For instance, Ga−In alloys and Ga−In−Sn alloys exhibit melting points of approximately 15 and −19 °C, respectively, remaining liquid at room temperature. Nonetheless, PVD of these alloyed liquid metals introduces additional challenges owing to their unique properties: they are composed of multiple metals, exhibit high surface tension, and their surfaces are prone to oxidation.[20,43−45] Gallium-based liquid metals, typically comprising two or three different metals, demonstrate separation and volatilization of each component during heating and evaporation, leading to realloying on the substrate surface[33] and resulting in nonuniform alloy growth. Furthermore, the formation of isolated microscopic particles, which are not electrically connected due to the high surface tension of liquid metals and the rapid formation of oxide films on their surfaces,[46] complicates the direct heat deposition of liquid metal on substrate surfaces. To overcome these obstacles and fulfill the specified requirements, a novel approach was developed to inhibit the formation of microparticles and ensure the adherence of deposited liquid metal to the substrate surface without the need for postphysical stimulation, such as applying pressure. This was achieved through the direct deposition of liquid metals on copper substrates that had been treated with copper chloride. The process involves a simple immersion of the vapor-deposited copper substrate into a $CuCl_2$ water solution, transforming the surface copper into CuCl. When chlorine ions come into contact with the oxide film on the liquid metal, the oxide film is transformed into a gallium chloride film. Gallium chloride is highly deliquescent, absorbing moisture from the air and turning it into an acidic solution.[47] In this study, this reaction occurs only with the substrate and liquid metal droplets through the direct generation of chlorides on the substrate surface. Therefore, this reaction is independent of the ambient air environment

The CuCl film effectively disrupts the oxide film on the surface of the liquid metal, preventing nanoparticle formation and enabling the liquid metal to uniformly spread and electrically connect across the substrate surface. The method used in this study does not require the fabrication of structures on the substrate surface in advance, nor does it require physical stimulation after the liquid metal film is formed. Therefore, liquid metal patterning can be performed with high accuracy while keeping the substrate surface clean. This is an advantage over conventional methods and is expected to be applicable in the future, for example, to liquid metal patterning on ultrathin films, biomaterials, and other materials vulnerable to physical stimulation, as well as to three-dimensional multilayer patterning of high-resolution liquid metal interconnections.

EXPERIMENTAL SECTION

Materials. $CuCl_2{\cdot}2H_2O$ (AR grade) was acquired from FUJIFILM Wako Pure Chemical Corporation. Galinstan, the liquid metal, was procured from Zairyo-ya.com. Copper and Chromium grains were sourced from Nilaco Corporation.

Copper Substrate Preparation. A controlled PVD technique was employed for the deposition of chromium and copper onto the substrate. Within the vacuum chamber, Cr and Cu grains were placed on a tungsten boat, respectively. The evaporator (EBX-6D, ULVAC) chamber's vacuum level was maintained below 2.0×10^{-3} Pa. Initially, a layer of chromium measuring 100 Å was deposited at a rate of 1 Å per second, followed by the deposition of 3 kÅ of copper at a rate of 50 Å per second. The thickness of the deposited film was monitored using a film thickness gauge (CRTM-6000G, ULVAC).

Surface Treatment. A $CuCl_2$ solution was prepared by dissolving 0.05 g of $CuCl_2{\cdot}2H_2O$ in 60 mL of deionized water. The substrate, coated with Cr and Cu layers, was immersed in this solution for 90 s and thereafter rinsed with water. Subsequently, water droplets were removed using a nitrogen blower.

Liquid Metal Deposition. Galinstan was deposited onto the treated substrate using a PVD technique. 0.2 mL of Galinstan was placed on the tungsten boat within the vacuum chamber, which was subsequently evacuated to under 2.0×10^{-3} Pa. A current of 150 A was applied for 5 min to evaporate all the liquid metal present on the boat.

OCP Measurement. A 10 nm adhesive layer of Cr and 300 nm copper were deposited on a silicon substrate, and copper tape (3 M Conductive Single Coated Copper Tape) was applied to the copper film, which was then fixed inside the container. A counter electrode and a reference electrode were also fixed in the container. These electrodes and the copper tape were connected to a potential measuring device (Meiden Hokuto HZ-7000). Copper chloride solution was added to the container, and OCP data were obtained by measuring the change in the potential of the copper tape immediately after the solution was added.

Electrical Resistance Measurement. A substrate on which copper and liquid metal were deposited was fixed to a one-axis horizontal moving motorized stage (Sigma Koki OSMS26-50), and an electrical resistance measuring instrument (Sanwa Electric Instrument Co. Digital Multimeter PC773) was connected to the substrate. The electrical resistance in the extended state was measured by extending it with a motorized stage controller (Sigma Koki Three-Axis Stage Controller HSC-103) and reading the value from the digital multimeter.

https://doi.org/10.1021/acsaelm.4c02096
ACS Appl. Electron. Mater. XXXX, XXX, XXX−XXX

Photolithography. Photoresist (Merck, AZ-1500) was spin-coated onto a substrate. The substrate was then heated at 90 °C for 1 min. A photomask was placed on the top surface of the substrate and irradiated with ultraviolet light for 30 s. The photoresist pattern was then developed in a developing solution (Tokyo Ohka Kogyo, NMD-3) for 5 min to obtain the photoresist pattern.

Characterization. The surface morphology of the sample was examined via a field-emission SEM (SU 8010, HITACHI). XPS (Quantera-SXM, ULVAC-PHI) was conducted to analyze the surface compositions and the chemical valence of surface elements. The reaction state of the substrate surface was assessed with a surface potential meter (HZ-7000, MEIDEN HOKUTO).

RESULTS AND DISCUSSION

In this study, we developed a method for fabricating electrically connected, gallium-based liquid metal (Gallinstan) thin layers through direct PVD. Gallinstan is an alloy of Ga:In:Sn = 68.5:21.52:10. This metal maintains its liquid state at room temperature by lowering the melting point of Ga through the addition of In and Sn.

This process involves the formation of a CuCl film on the substrate's surface (Figure 1a) that interacts with the oxide film

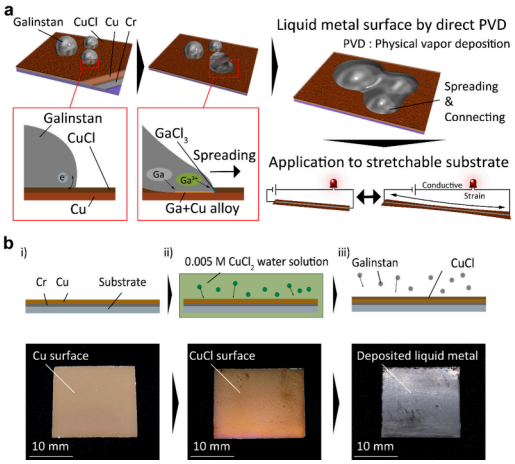

Figure 1. Concept of direct physical deposition of liquid metal on CuCl-treated substrates. (a) Schematic of the wetting and spreading of liquid metal deposited on copper chloride. The liquid metal film fabricated by this method can be used for various applications, including stretchable substrates and integration with lithography technologies. (b) Substrate surface image acquired during CuCl treatment and liquid metal deposition.

on the liquid metal surface, disrupting the oxide layer and allowing gallium to alloy with the copper on the substrate. This reaction proceeds continuously, leading to the gradual wetting of the liquid metal on the substrate, thereby causing the previously isolated nanoparticles to spread and become electrically connected. The resulting liquid metal film can be directly applied to stretchable substrates, offering a novel approach to fabricating wiring patterns by integrating various pattern fabrication technologies, such as photolithography. First, chromium and copper film were deposited on the substrate surface by vapor deposition (Figure 1b(i)). The chromium improves adhesion between the substrate and the copper. Second, the substrate was immersed in a copper(II) chloride water solution (Figure 1b(ii)). Subsequently, a liquid metal vapor deposition film is formed on the substrate through physical vapor deposition (PVD) of the liquid metal (Figure 1b(iii)).

Figure 2a illustrates the surface of the Si substrate and scanning electron microscopy (SEM) images of the liquid metal deposited directly without a copper chloride film. The interactions between atoms in liquid metals are stronger than those between atoms and substrates due to the high surface energy of liquid metals, which leads to film formation according to the Volmer–Weber mechanism.[48] Furthermore, since the liquid metal used in this study is an alloy of several metals with different melting points, alloy separation and realloying occur during deposition. During realloying, liquid metal nuclei are generated on the substrate surface, and liquid metal particles grow from these nuclei. In this film formation mechanism, film growth is nonuniform, and localized film formation occurs across the substrate, resulting in the absence of electrical connectivity between the particles. Consequently, the substrate's surface remains nonconductive. The generation of particles by liquid metal has been extensively researched, demonstrating that similar microparticles are produced when EGaIn (a gallium–indium alloy) is deposited.[33] Both Galinstan and EGaIn, being alloys comprising various metals with differing melting points, undergo individual metal evaporation and subsequent reformation of alloy nuclei on the substrate during resistance heating evaporation. Subsequent adhesion and growth of additional liquid metal on the nucleus surface occur. Given the exceedingly high surface energy of liquid metal, the formation of individual isolated particles follows the Volmer–Weber mechanism.[48] According to this theory, a film of liquid metal gradually grows and coalesces on the substrate surface. When it reaches a certain size, the metals stop interacting with each other and grow as independent particles. Therefore, microparticles of liquid metals are generated even in high vacuum deposition environments.

Figure S1 shows a more detailed SEM image of the liquid metal particles formed on a copper film without copper chloride treatment. The liquid metal forms spherical particles and does not exhibit the spreading observed in Figure 2b. These particles grow according to the Volmer–Weber mechanism[48] in a vacuum and lose their surface conductivity due to the oxide film when exposed to air. Therefore, it is necessary to remove the microparticles generated on the substrate.

Film formation in the Volmer–Weber mode is a mechanism that occurs when the interaction among the deposited atoms exceeds the interaction between the adsorbed atoms and the substrate surface. In this mechanism, film formation becomes random, and independent islands are formed when the film thickness exceeds a specific threshold. Therefore, it is necessary to ensure sufficient interaction between the liquid metal and the substrate surface to enhance the wettability of the liquid metal and form a conductive path.

To address this issue, previous research proposed increasing the contact area between the liquid metal and the substrate by fabricating micropillars to enhance the interaction of the substrate with the liquid metal.[30] In this study, the formation of particles is suppressed by the interaction between the micropillars and the liquid metal; however, this is not applicable to substrates that do not readily support the formation of micropillars. Conversely, the methodology proposed in this study does not require any substrate material, and direct deposition of liquid metal is possible without prior mechanical treatment on suitable substrates.

Moreover, the propensity of liquid metal to form an oxide film on its surface leads to each particle being encapsulated by

https://doi.org/10.1021/acsaelm.4c02096
ACS Appl. Electron. Mater. XXXX, XXX, XXX−XXX

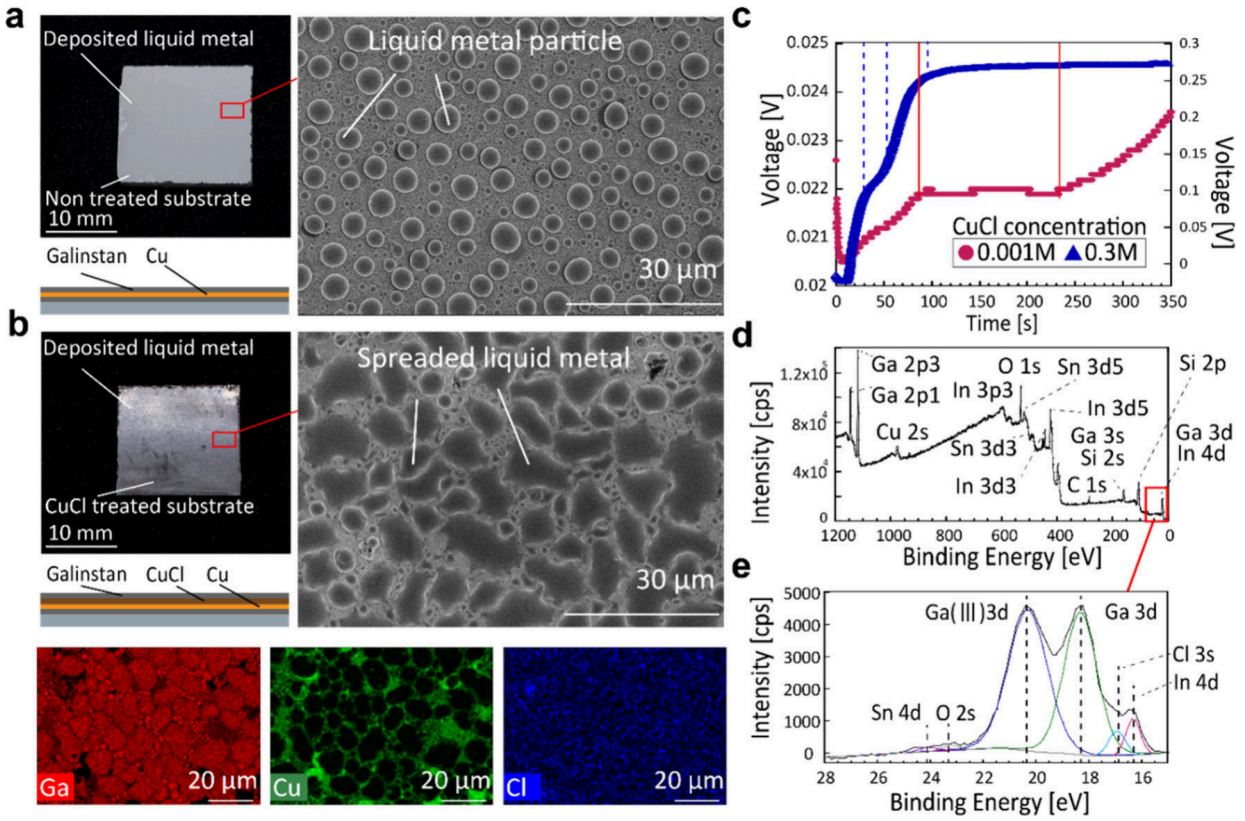

Figure 2. Surface properties of copper chloride treatments and liquid metal deposition. (a) Surface of the Si substrate with SEM images illustrating liquid metal deposited directly without a copper chloride film, where electrical connections are disrupted due to the presence of independent liquid metal nanoparticles. (b) SEM and EDS images of liquid metal deposited on a substrate treated with CuCl, illustrating how the liquid metal spreads and interconnects. (c) Results from OCP analysis indicating the Cu surface reacts with $CuCl_2$ water solution in two distinct steps. (d,e) XPS analysis results of the liquid metal-deposited substrate surface, revealing the presence of gallium in oxide, chloride, and metallic states.

an insulating oxide film, thereby preventing electrical connectivity even upon contact between particles. The extremely high surface tension of liquid metal hinders the simple coalescence of the particles upon contact. An activation process is necessary to sufficiently press the particles together, either by magnetic force,[49] heating with a laser,[26] or pressure with a stylus.[50] However, activation by magnetic force limits the size and shape of the liquid metal wiring that can be formed. Additionally, the laser and needle methods require a mechanical activation process after film formation, which often damages the substrate surface and limits the substrate materials that can be used. By contrast, this research does not require any physical activation process on the substrate surface, thus maintaining a clean substrate surface and offering a wide choice of substrates.

Figure 2b presents an image of a substrate with liquid metal deposited atop a copper chloride film, accompanied by SEM images and EDS analysis results. The SEM images indicate that the liquid metal particles are disrupted by their interaction with the copper chloride film, resulting in their spread across the surface in a liquid state, which facilitates electrical connectivity and conduction by the liquid metal. EDS analysis reveals a widespread distribution of chloride on the surface, with Ga also exhibiting widespread wetting and spreading. The removal of oxide films from liquid metals is known to employ hydrochloric acid and hydrogen chloride gas, as chloride ions from hydrogen chloride transform the oxide film into a chloride film.[51]

This study constructs a bilayer structure of copper and copper chloride on the substrate surface, enabling the liquid metal to contact the copper chloride surface, thereby simultaneously removing the oxide film and spreading in a liquid state. The copper chloride film on the substrate surface facilitates the wetting and spreading process of the liquid metal by alloying with the copper substrate and inhibiting the formation of an oxide film. A study examining the exposure of Gallinstan to hydrogen chloride gas[51] reported that chlorine ions degrade the oxide film on the surface of the liquid metal by replacing it with a chloride film. Owing to its high tidal solubility,[47] the chlorine film absorbs moisture from the air and converts it into an aqueous solution, thereby losing its function as a film. In this study, copper chloride was formed on the substrate surface as a source of chloride ions instead of gaseous chloride.

Additionally, Galinstan does not readily alloy with copper, and previous studies that tested the mixing of these two metals after removing their oxide films[52] have not confirmed reactive wetting due to the surface tension of the liquid metal. In addition to the removal of the surface oxide film, a small amount of acidic water containing chlorine ions is required[53] for the liquid metal to alloy with the copper surface. Alloying of copper and liquid metal does not occur in a vacuum deposition environment.

Therefore, to fully alloy Gallinstan and copper and generate reactive wetting, it is necessary to remove the oxide film on the surface of the Gallinstan by introducing chlorine ions in an atmosphere containing moisture, and bringing the copper into

https://doi.org/10.1021/acsaelm.4c02096
ACS Appl. Electron. Mater. XXXX, XXX, XXX−XXX

contact with liquid metal. This study's film formation mechanism is as follows: The liquid metal grown under vacuum conditions has a particle shape, and when exposed to air, an oxide film rapidly grows to cover the surface. Subsequently, the oxide film is disrupted by moisture in the air and chlorine ions on the substrate surface, allowing the liquid metal to further alloy with copper through the action of an acidic solution.

In a previous study that measured the decrease in contact angle due to the reaction between liquid metal and copper chloride film,[53] a decrease in contact angle was observed in both cases within the range of 13 to 65% humidity. The study reported that the contact angle decreased to about 20° within approximately 5 min at humidity levels of 20% or higher. In this study, no special environmental humidity control was implemented, but the humidity in the test environment was maintained above about 50%, which was assumed to have no effect on wettability.

The interactions occurring upon copper chloride contact with Ga have been previously reported[53] (eq 1).

$$Ga + 3CuCl \rightarrow GaCl_3 + 3Cu \quad (1)$$

The gradual absorption of moisture from the air by $GaCl_3$ results in the formation of a thin film of aqueous copper chloride solution on the liquid metal surface.[54] This solution's acidity, stemming from the hydrolysis reaction of $GaCl_3$, facilitates the removal of the oxide film on the gallium surface and dissolves CuCl through subsequent reactions (eq 2).

$$CuCl + 2Cl^- \rightarrow [CuCl_3]^{2-} \quad (2)$$

In addition, gallium reduces copper ions to form elemental copper by the following reaction (eq 3).

$$Ga + 3[CuCl_3]^{2-} \rightarrow Ga^{3+} + 3Cu + 9Cl^- \quad (3)$$

The copper deposited through this process undergoes intermittent alloying by gallium phagocytosis,[55] facilitating the spreading of liquid metal over the substrate surface and preventing the formation of nanoparticles.

A previous report[53] demonstrated that chloride ions and a small amount of acidic solution are required on the liquid metal surface to destroy microparticles and promote alloying with the substrate surface. Chloride ions are generated when the oxide film on the liquid metal surface reacts with copper chloride. In other words, the oxide film reacts with CuCl and not the liquid metal itself. Acidic solutions are formed when the chloride film absorbs moisture from the air. The particles are destroyed and spread on the substrate surface when both chloride ions and acidic solutions act on the microparticles. Therefore, to destroy the microparticles formed by the process used in this study and improve wettability, it is necessary to first form an oxide film on the surface by exposure to air, then react this film with chloride ions, and finally absorb moisture from the air. In this study, this series of processes is accomplished by using copper chloride coated on the substrate surface. A chloride film must be formed once and then exposed to moisture in the air to ensure sufficient wettability, and it is considered that enough wettability is not achieved under vacuum conditions during the deposition process.

In the study by Wang et al., a $CuGa_2$ shell was formed by mixing Cu and GaInSn.[56] In this study, NaOH was added to remove the oxide film. Both chloride and hydroxide ions are known to destroy the oxide film on the surface of liquid metals,[57] which may play the same role as CuCl in this study.

Additionally, regarding the wettability between liquid metal and the substrate surface, there are reports that substrate surface roughness improves wettability.[31] Previous studies have shown that treatment of copper surfaces with copper chloride results in the formation of a rough film on the surface.[53] According to this study, protrusions formed on the substrate surface by the reaction of copper chloride with copper are approximately 0.5−2 μm in size. The liquid metal particles formed in this study are approximately 0.2−1 μm in diameter, which is nearly the same size as the protrusions on the substrate surface. The diameter ratio of the protrusions on the substrate surface to the diameter of the liquid metal was approximately 1000 in research,[31] which improved the wettability of liquid metal by roughening the substrate surface. In research,[29] which improved wettability by forming a three-dimensional structure on the substrate surface, the diameter ratio was approximately 40. In comparison to these studies, the diameter ratio of the droplet to the substrate surface structure in this study is smaller, suggesting that chemical reactions are more dominant than surface roughness.

Figure 2c presents the open circuit potential (OCP) measurement results during the formation of the copper chloride film. In this experiment, a copper(I) chloride film was generated on the surface of a thin copper film by immersion in a copper(II) chloride aqueous solution, as depicted below (eq 4).

$$Cu + CuCl_2 \rightarrow 2CuCl \quad (4)$$

Excessive immersion of this substrate in the solution leads to a reaction with water, resulting in the redeposition of copper(II) chloride[53] (eq 5).

$$12CuCl + 6H_2O + 3O_2 \rightarrow 4Cu_2(OH)_3Cl + 4CuCl_2 \quad (5)$$

For this measurement, two different concentrations of copper chloride solutions (0.001 M, 0.3 M) were employed to observe changes in surface potential. The results, as illustrated in the graphs, indicate a two-phase potential change in both instances. Initially, copper is converted to copper(I) chloride. Subsequently, an equilibrium state is reached between reactions 4 and 5. Ultimately, the reaction described in reaction 5 predominates, converting the entire surface to copper(II) chloride. The reaction concludes when the entire accessible area is covered with copper(II) chloride and the potential stabilizes. Steps on the copper and copper chloride surfaces were measured with a stylus-type film thickness meter for 30, 60, 120, 180, and 300 s immersion times. The results are shown in Figure S2. Notably, the increase in film thickness decreases after approximately 120 s. It is beyond this point that the reaction in which copper chloride I is converted to copper chloride II is considered to have occurred, with the film thickness reaching equilibrium.

Thus, to adequately form a copper(I) chloride film on the surface, optimizing the concentration and immersion time of the copper(I) chloride solution is imperative. Given this context, a sufficiently thick copper chloride I film was required; thus, the immersion time was set to 90 s before the formation of the copper chloride II film.

Figure S3 illustrates the temporal progression of a copper substrate immersed in a 0.001 M copper chloride solution. Initially, the substrate reacts with the solution to form a brown

https://doi.org/10.1021/acsaelm.4c02096
ACS Appl. Electron. Mater. XXXX, XXX, XXX−XXX

copper chloride(I) film on its surface. Prolonged immersion eventually leads to the formation of a green copper chloride(II) film. Given the differential reactivity of copper chloride(I) and copper chloride(II) with liquid metal surfaces, preparing a surface with exclusively copper chloride(I) is crucial. Figure S4a displays the contact angle of a Galinstan droplet on a copper chloride(I) film, demonstrating a gradual decrease in the contact angle to approximately 1° after 120 s. Conversely, Figure S4b shows similar observation results when a droplet was placed on a $CuCl_2$ film, revealing that the $CuCl_2$ film does not interact with the liquid metal surface, resulting in the persistence of the droplet form and lack of spreading.

Figure 2d presents the findings from X-ray photoelectron spectroscopy (XPS) analysis of the substrate surface, with visible Ga 2p and Ga 3p peaks around 1200 eV, indicating oxidation of the liquid metal on the substrate surface.[51] Peaks corresponding to Si 2s, Si 2p, and C 1s, attributable to the silicone resin of the substrate material, alongside the Cu 2 peak from copper on its surface, were also observed. Figure 2e offers a detailed view around 20 eV, enabling estimation of the chemical bonding state of gallium within the liquid metal.[53] The peak around 18 eV correlates with elemental gallium, and the peak around 20.3 eV is presumed to represent Ga^{3+}. These findings suggest the coexistence of gallium ions in oxide film form and single-metal gallium on the substrate surface. Peaks around 16−17 eV are ascribed to In and Cl, indicating their distribution on the surface due to Cl's presence on the copper chloride surface and In's role as a component of Gallinstan. Additionally, two peaks around 23 eV, attributed to O and Sn, were observed, with Sn constituting approximately 10% of Galinstan and O likely forming an oxide film on the surface.

Subsequently, liquid metal deposition was employed to a stretchable substrate. Figure 3a presents both a photograph and the SEM observation results of a polydimethylsiloxane (PDMS) substrate with gallinstan deposited onto a copper and copper chloride film. The SEM imagery elucidates how gallinstan serves as a conduit across the copper film, effectively bridging the gaps through its spread. This particular substrate has been engineered to endure an extension of up to approximately 30%. Figure S5 shows SEM images of a copper chloride film and deposited liquid metal on a PDMS substrate before stretching. Notably, the liquid metal is wetted and spread on the substrate without strain, forming a connection with the adjacent particles. Conversely, the liquid metal film deposited on PDMS retains more droplets than on the silicon substrate surface. This phenomenon can be due to the roughness of the PDMS surface, which has many nanometer-order ruggedness. This affects the contact area between the liquid metal and the substrate, potentially resulting in additional droplet formation.

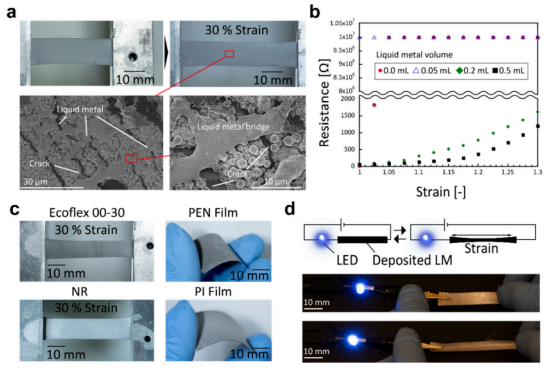

Figure 3. Characteristics of liquid metal films deposited directly on stretchable and flexible substrates. (a) Photographs and SEM images presenting liquid metal deposited on a PDMS substrate, where the wet-spread liquid metal cross-links the cracks within the copper substrate. (b) Changes in electrical resistance under strain, with measurements acquired for varying amounts of liquid metal subjected to strains up to 30%. (c) Application of liquid metal deposition on various substrate materials, demonstrating the adherence of vapor-deposited liquid metal to multiple types of substrates. (d) Demonstration of LED lighting, showing an LED powered and illuminated even when the liquid metal wiring is stretched by approximately 30%.

Figure 3b delineates the electrical resistance measurements of the substrate when subjected to strain. This evaluation was conducted by modulating the volume of liquid metal deposited, with variations including the absence of liquid metal, 0.05, 0.2, and 0.5 mL, respectively. During the measurements, both substrates were connected in parallel to a fixed 10 MΩ resistor. Given the nonconductive nature of copper chloride (referenced in Figure S6), electrical conductivity remains undetected at minimal liquid metal volumes. Conversely, a deposition of liquid metal (>0.2 mL) on the surface ensures the maintenance of electrical conductivity, even after 30% elongation. Notably, the electrical resistance decreases as the amount of liquid metal increases, indicative of enhanced electrical conductivity. Nonetheless, a limitation arises with an overly thin copper chloride film, necessitating an optimized thickness to accommodate increased volumes of liquid metal.

A previous study[53] reported the use of thicker copper foil and a high concentration of copper chloride solution (0.5 mol L^{-1}). In this method, liquid metal film formation is achieved by direct drop deposition rather than vapor deposition. The size of the droplets in this study was about 1 mm in diameter, and the film thickness was several tens of micrometers, which is much thicker than the liquid metal film produced in this study (approximately 1.3 μm). Therefore, the thickness of the liquid metal film can be controlled by the copper film on the substrate, the concentration of the copper chloride solution, and the size of the liquid metal particles. Additionally, studies on the formation of liquid metal particles[46] through evaporation have reported that the size of the liquid metal particles varies with the evaporation rate. Based on these results, it is believed that the reaction between the liquid metal particles and the copper chloride film can be controlled by optimizing the deposition rate of the liquid metal, in addition to adjusting the copper film and copper chloride concentration, thereby altering the thickness of the film.

To verify the effect of copper chloride, a similar tensile test was conducted by depositing liquid metal on copper without copper chloride treatment (Figure S7). The resistance of the substrate without copper chloride treatment increased rapidly when the tensile strength exceeded 0.3%, reaching 10 MΩ, the same as the fixed resistance of the parallel-connected substrate. This is considered to be due to the copper film being only conductive, with slight elongation causing the copper film to crack, resulting in the loss of electrical conductivity.

Figure S8 illustrates the variance in electrical resistance following 30 cycles of 30% strain, where a progressive increase in electrical resistance is observed, culminating in a loss of conductivity after 30 stretching cycles. This phenomenon is attributed to the formation of cracks within the copper film

https://doi.org/10.1021/acsaelm.4c02096
ACS Appl. Electron. Mater. XXXX, XXX, XXX−XXX

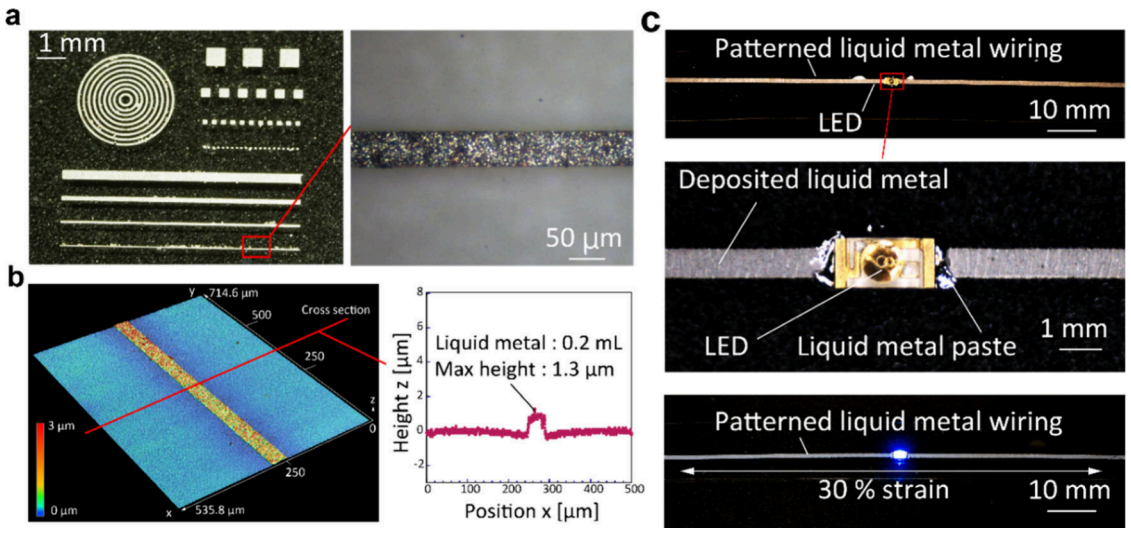

Figure 4. Various pattern fabrication and applications of top surface electric components. (a) Liquid metal patterned via the photolithography technique, demonstrating the capability to form various shapes, including distinct areas. (b) Measurement of liquid metal line thickness via laser microscopy, with a thickness of approximately 1.3 μm; areas outside of the wiring remain flat. (c) Demonstration of an LED on the patterned and deposited liquid metal.

upon each deformation, eventually surpassing the liquid metal's capability to bridge these gaps. Enhancing the stability of repeatability may be achievable through the fine-tuning of both the liquid metal volume and the copper layer's thickness.

Figure 3c exhibits substrates subjected to liquid metal vapor deposition across various materials. Materials deposited via PVD exhibit superior adhesion to substrate surfaces. Consequently, a broad spectrum of substrate[58] materials is viable for deposition. Gallinstan was deposited using PVD on Ecoflex 00-30 and natural rubber (NR) sheet as stretchable substrates, and on polyethylene naphthalate (PEN) film and polyimide (PI) film as flexible substrates. Ecoflex is widely used for substrates that undergo significant deformation because of its high elasticity and low Young's modulus. Natural rubber is also widely used for devices that require hermetic sealing owing to its high availability and low gas permeability. The fabrication of stretchable interconnections in these materials is crucial for developing a wide range of stretchable devices. However, the electrical resistance of the liquid metal on Ecoflex 00-30 and NR is higher than that deposited on PDMS, and the elongation ratio is low, at approximately 5% for Ecoflex and approximately 20% for NR (Figure S9a). This is thought to be primarily due to modification of the substrate surface by the heat of deposition. In particular, Ecoflex is known to have low heat resistance and is prone to thermal expansion. When the deposition source and substrate are close, the surface expands due to the temperature of resistance heating, making it difficult to form a uniform metal film. To address this challenge, a large evaporator with a long distance between the evaporation source and the substrate, or an evaporator equipped with a substrate cooling system, can be used. Additionally, a more stable liquid metal film can be formed by thickening the first-layer copper film to minimize the effects of thermal deformation.

Additionally, among flexible substrates, PEN film with high transparency, and PI film with high heat and chemical resistance, are widely used as materials for flexible devices. Electrical conductivity was also measured on PEN and PI (Figure S9b). Conductivity was stable on both PEN and PI surfaces. This is because the substrates were not stretched and conducted not only to the liquid metal but also to the copper film on the bottom layer. These substrates are often combined with stretchable materials when rigid electronic components are mounted on stretchable substrates. Therefore, the ability to form liquid metal films with high adhesion on these substrates is essential for wiring technologies in stretchable devices.

These stretchable substrates demonstrated an elasticity of approximately 30% without detachment from the substrate, while the flexible substrates could be bent to a radius of 3 mm without any observed delamination (as depicted in Figure S10).

Figure 3d illustrates the outcomes of an LED lighting experiment conducted as a demonstrative application. A blue LED connected to a power supply via liquid metal wiring was illuminated upon voltage application. Remarkably, the LED continued to illuminate even when the substrate was stretched by approximately 30%, signifying that the circuit preserved adequate electrical conductivity even under strain. Torsional and bending deformations were applied in addition to the elongation test (Figure S11). The liquid metal film on PDMS adhered strongly to the substrate, preventing delamination during the deformations. In both cases, the LEDs remained functional under deformation.

A test was conducted to evaluate the efficacy of PVD for patterning liquid metal on a substrate surface. PVD offers superior control over film thickness compared with other liquid metal layer fabrication techniques and facilitates patterning through various methods, including photolithography. Figure 4a illustrates a substrate surface patterned using both photolithography and PVD, demonstrating the feasibility of creating patterns of arbitrary shapes through the combination of these techniques.

A previous study[53] proposed a method to achieve liquid-metal film formation and patterning by directly applying liquid metal after CuCl treatment. Compared to vapor deposition, the total number of steps in this method is fewer than that of the simple coating process. However, the copper film on the substrate in the study must be several hundred μm thick, and the thickness of the liquid metal was several tens of μm. The total film thickness, from the substrate surface to the top of the

https://doi.org/10.1021/acsaelm.4c02096
ACS Appl. Electron. Mater. XXXX, XXX, XXX−XXX

liquid metal film, was in the hundreds of μm. Since photoresists for photolithography are generally in the range of μm to tens of μm thick, it is difficult to pattern the liquid metal film formed with this thickness by photolithography. When patterning with liquid metal film by direct application, a wiring pattern is created on the substrate using adhesive tape in advance. Subsequently, CuCl-treated copper particles are sprayed onto the adhesive tape, and liquid metal is deposited from the top surface. Since this method requires patterning with adhesive tape, achieving fine and complex patterns is challenging; however, it can be achieved by photolithography. The liquid metal deposition process proposed in this study has the advantage of being easily combined with thin-film fine patterning techniques because it can form thinner films than coating.

The results of laser film thickness measurements for the patterned lines, presented in Figure 4b, indicate a film thickness of approximately 1 μm, with the top surface of the film remaining uniformly flat at the microscale. Furthermore, the areas of the substrate surface not covered by wiring remained clean, with negligible excess material observed.

Various techniques for patterning liquid metal have been proposed, such as direct flow into microchannels,[17−19] stencil printing,[20−23] imprinting,[28] direct deposition using a dispenser,[24,25] and nanoparticle sintering printing by a laser.[26,27] The characteristics of each method are summarized in Table 1.

Table 1. Comparison of Processing Methods

	top surface	thickness	pattern design	surface cleanness
microchannels[17−20]	not-opened	10−50 μm	limited	sealed surface
stencil printing[21−23]	opened	3−10 μm	limited	clean
imprinting[28]	not-opened	∼1 μm	unlimited	contact with another substrate
dispensing[24,25]	opened	100−500 μm	unlimited	clean
laser sintering[26,27]	opened	10−20 μm	unlimited	excess particles on the surface
this study	opened	∼1 μm	unlimited	clean

The microfluidic method poses challenges for placing electronic elements on the substrate, as the microfluidic channels are completely sealed by the substrate material. Moreover, creating independent wiring areas is problematic, necessitating the fabrication of liquid metal inlets and outlets for all wiring. Stencil printing requires precise alignment of multiple masks to create independent wiring areas, presenting technical difficulties. Imprinting involves transferring liquid metal from another substrate, which compromises the cleanliness of the substrate surface, as the entire top surface comes into contact with another substrate during the process. Dispensing printing struggles to achieve fine lines due to the difficulty in producing thin layers, and the precision of the pattern edges is compromised by the liquid metal's high surface tension. Laser sintering necessitates spraying the entire surface with a liquid metal nanoparticle solution, increasing the risk of unintended conduction and compromising the cleanliness of the surface. The direct PVD technique addressed in this study mitigates these issues, offering several advantages including an open top surface for direct mounting of electronic elements, the capability to employ a broad spectrum of patterning techniques such as lithography for achieving arbitrary shapes, and the maintenance of a clean substrate surface postwiring.

Figure 4c depicts the direct attachment of an electronic component, specifically an LED, onto a line pattern engineered on a substrate that has been stretched, utilizing the film stencil technique. The wiring pattern, deposited via vapor deposition, is characterized by its flatness and openness at the top surface, which simplifies the process of directly mounting small components. For the connection between the wiring and the component, a conductive mixture containing gallinstan and nickel powder is utilized to ensure conductivity even when the substrate is under strain. This particular substrate can be extended by approximately 30%. The LED remained illuminated upon the application of voltage, despite the substrate's elongation. The fabricated thin films of liquid metal in this study can be used with various patterning techniques, such as photolithography and stencil printing, to create wiring patterns with a wide range of shapes. This ability may enable the construction of various wiring structures on stretchable substrates, which are currently fabricated by vapor deposition processes. Additionally, the use of specific substrate materials to mount rigid electronic elements on a stretchable substrate[59,60] will enable the fabrication of various high-functional stretchable devices such as stretchable display devices and wearable electrocardiographs.

CONCLUSIONS

In this study, the wettability between liquid metal and the substrate was significantly enhanced by treating the substrate surface with copper chloride, facilitating the successful fabrication of wiring through the direct PVD of liquid metal. The presence of copper chloride on the substrate surface effectively disrupted the oxide film on the liquid metal, promoting interconnectivity between liquid metal particles and thereby preserving conductivity even when subjected to 30% strain. This advancement enabled powering LED elements under strain through the wiring. The methodology employed can be integrated with various wiring patterning techniques, including patterning achieved through photolithography. Moreover, electronic components can be directly mounted on the thus fabricated wiring and operated under strain, attributed to the wiring's open top surface. However, the repeatability of this process poses a challenge, which could be improved by optimizing the surface treatment conditions and deposition parameters. Given the fine and thin nature of the stretchable wiring produced by this method, its application is anticipated in higher-density devices employing more advanced integration methods, such as 3-dimensional multilayer wiring. Furthermore, the potential exists to create stretchable devices of heightened functionality by combining this technique with technologies that enable the mounting of rigid electronic elements on stretchable substrates.

ASSOCIATED CONTENT

Supporting Information

The Supporting Information is available free of charge at https://pubs.acs.org/doi/10.1021/acsaelm.4c02096.

Detailed SEM image of the microparticle, graph of $CuCl_2$ layer thickness, photograph of copper substrate surface, photograph of changing contact angle of liquid

https://doi.org/10.1021/acsaelm.4c02096
ACS Appl. Electron. Mater. XXXX, XXX, XXX−XXX

metal, SEM images of deposited liquid metal on PDMS substrate before stretched, electrical resistance between Cu and CuCl, changes in electrical resistance under tensile strain without CuCl treatment, strain repeatability test results, changes in electrical resistance on Ecoflex, NR, PEN, and PI films, flexible substrate curvature test results, torsional and bending deformation demonstrations (PDF)

AUTHOR INFORMATION

Corresponding Authors

Hiroki Ota − *Department of Mechanical Engineering and Institute for Multidisciplinary Sciences, Yokohama National University, Yokohama 240-8501, Japan; Graduate School of System Integration, Yokohama National University, Yokohama 240-8501, Japan;* orcid.org/0000-0002-3702-6357; Email: ota-hiroki-xm@ynu.ac.jp

Fumihiro Inoue − *Faculty of Engineering and Institute for Multidisciplinary Sciences, Yokohama National University, Yokohama 240-8501, Japan;* orcid.org/0000-0003-2292-846X; Email: inoue-fumihiro-ty@ynu.ac.jp

Authors

Ryosuke Matsuda − *Department of Mechanical Engineering, Yokohama National University, Yokohama 240-8501, Japan;* orcid.org/0009-0009-4667-3036

Yuji Isano − *Department of Mechanical Engineering, Yokohama National University, Yokohama 240-8501, Japan*

Koki Onishi − *Department of Mechanical Engineering, Yokohama National University, Yokohama 240-8501, Japan*

Complete contact information is available at: https://pubs.acs.org/10.1021/acsaelm.4c02096

Author Contributions

The manuscript was written through contributions of all authors. All authors have given approval to the final version of the manuscript. H.O. and F.I. contributed equally to this study and share joint corresponding authorship.

Notes

The authors declare no competing financial interest.

ACKNOWLEDGMENTS

This work was supported by JSPS KAKENHI grant no. JP22KJ1407, JSPS KAKENHI grant no. 23K26388, and Japan Science and Technology Agency (JST) Advanced Integrated Intelligence Platform Project (no. JPMJCR22U2).

ABBREVIATIONS

PVD, physical vapor deposition; SEM, scanning electron microscopy; EDS, energy dispersive spectroscopy; OCP, open circuit potential; XPS, X-ray photoelectron spectroscopy; PDMS, polydimethylsiloxane; EGaIn, eutectic gallium−indium; NR, natural rubber; PEN, polyethylene naphthalate; PI, polyimide; $CuCl_2$, copper(II) chloride; CuCl, copper(I) chloride; $GaCl_3$, gallium(III) chloride

REFERENCES

(1) Gao, W.; Emaminejad, S.; Nyein, H. Y. Y.; Challa, S.; Chen, K.; Peck, A.; Fahad, H. M.; Ota, H.; Shiraki, H.; Kiriya, D.; Lien, D. H.; Brooks, G. A.; Davis, R. W.; Javey, A. Fully Integrated Wearable Sensor Arrays for Multiplexed in Situ Perspiration Analysis. *Nature* **2016**, *529* (7587), 509−514.

(2) Wicaksono, I.; Tucker, C. I.; Sun, T.; Guerrero, C. A.; Liu, C.; Woo, W. M.; Pence, E. J.; Dagdeviren, C. A Tailored, Electronic Textile Conformable Suit for Large-Scale Spatiotemporal Physiological Sensing in Vivo. *npj Flexible Electronics* **2020**, *4* (1), 5.

(3) Chen, L. Y.; Tee, B. C. K.; Chortos, A. L.; Schwartz, G.; Tse, V.; Lipomi, J. D.; Wong, H. S. P.; McConnell, M. V.; Bao, Z. Continuous Wireless Pressure Monitoring and Mapping with Ultra-Small Passive Sensors for Health Monitoring and Critical Care. *Nat. Commun.* **2014**, *5*, 5028.

(4) Xiao, C.; Zhang, H.; Zhao, H.; Xu, H.; Huang, J.; Zhou, T. Preparation of Liquid Metal Circuits on Flexible Polymers by Selective Laser Ablation: Essential Mechanism of Non-Conductivity in Ablation Part. *Appl. Surf. Sci.* **2022**, *605*, No. 154746.

(5) Kang, K.; Jung, H.; An, S.; Baac, H. W.; Shin, M.; Son, D. Skin-like Transparent Polymer−Hydrogel Hybrid Pressure Sensor with Pyramid Microstructures. *Polymers (Basel)* **2021**, *13* (19), 3272.

(6) Lipomi, D. J.; Vosgueritchian, M.; Tee, B. C. K.; Hellstrom, S. L.; Lee, J. A.; Fox, C. H.; Bao, Z. Skin-like Pressure and Strain Sensors Based on Transparent Elastic Films of Carbon Nanotubes. *Nat. Nanotechnol* **2011**, *6* (12), 788−792.

(7) Kabiri Ameri, S.; Ho, R.; Jang, H.; Tao, L.; Wang, Y.; Wang, L.; Schnyer, D. M.; Akinwande, D.; Lu, N. Graphene Electronic Tattoo Sensors. *ACS Nano* **2017**, *11* (8), 7634−7641.

(8) Miriyev, A.; Stack, K.; Lipson, H. Soft Material for Soft Actuators. *Nat. Commun.* **2017**, *8* (1), 596.

(9) Wehner, M.; Truby, R. L.; Fitzgerald, D. J.; Mosadegh, B.; Whitesides, G. M.; Lewis, J. A.; Wood, R. J. An Integrated Design and Fabrication Strategy for Entirely Soft. *Autonomous Robots. Nature* **2016**, *536* (7617), 451−455.

(10) Xie, Z.; Domel, A. G.; An, N.; Green, C.; Gong, Z.; Wang, T.; Knubben, E. M.; Weaver, J. C.; Bertoldi, K.; Wen, L. Octopus Arm-Inspired Tapered Soft Actuators with Suckers for Improved Grasping. *Soft Robot* **2020**, *7* (5), 639−648.

(11) Shepherd, R. F.; Ilievski, F.; Choi, W.; Morin, S. A.; Stokes, A. A.; Mazzeo, A. D.; Chen, X.; Wang, M.; Whitesides, G. M. Multigait Soft Robot. *Proc. Natl. Acad. Sci. U. S. A.* **2011**, *108*, 20400−20403.

(12) Jeong, Y. R.; Kim, J.; Xie, Z.; Xue, Y.; Won, S. M.; Lee, G.; Jin, S. W.; Hong, S. Y.; Feng, X.; Huang, Y.; Rogers, J. A.; Ha, J. S. A Skin-Attachable, Stretchable Integrated System Based on Liquid GaInSn for Wireless Human Motion Monitoring with Multi-Site Sensing Capabilities. *NPG Asia Mater.* **2017**, *9* (10), No. e443.

(13) Tang, S. Y.; Khoshmanesh, K.; Sivan, V.; Petersen, P.; O'Mullane, A. P.; Abbott, D.; Mitchell, A.; Kalantar-Zadeh, K. Liquid Metal Enabled Pump. *Proc. Natl. Acad. Sci. U. S. A.* **2014**, *111* (9), 3304−3309.

(14) Park, Y. L.; Chen, B. R.; Wood, R. J. Design and Fabrication of Soft Artificial Skin Using Embedded Microchannels and Liquid Conductors. *IEEE Sens. J.* **2012**, *12* (8), 2711−2718.

(15) Chen, J.; Zhang, J.; Luo, Z.; Zhang, J.; Li, L.; Su, Y.; Gao, X.; Li, Y.; Tang, W.; Cao, C.; Liu, Q.; Wang, L.; Li, H. Superelastic, Sensitive, and Low Hysteresis Flexible Strain Sensor Based on Wave-Patterned Liquid Metal for Human Activity Monitoring. *ACS Appl. Mater. Interfaces* **2020**, *12* (19), 22200−22211.

(16) Choi, D. Y.; Kim, M. H.; Oh, Y. S.; Jung, S. H.; Jung, J. H.; Sung, H. J.; Lee, H. W.; Lee, H. M. Highly Stretchable, Hysteresis-Free Ionic Liquid-Based Strain Sensor for Precise Human Motion Monitoring. *ACS Appl. Mater. Interfaces* **2017**, *9* (2), 1770−1780.

(17) Zhu, S.; So, J. H.; Mays, R.; Desai, S.; Barnes, W. R.; Pourdeyhimi, B.; Dickey, M. D. Ultrastretchable Fibers with Metallic Conductivity Using a Liquid Metal Alloy Core. *Adv. Funct Mater.* **2013**, *23* (18), 2308−2314.

(18) Cheng, S.; Wu, Z. Microfluidic Electronics. *Lab Chip* **2012**, *12*, 2782−2791.

(19) Fassler, A.; Majidi, C. Soft-Matter Capacitors and Inductors for Hyperelastic Strain Sensing and Stretchable Electronics. *Smart Mater. Struct.* **2013**, *22* (5), No. 055023.

(20) Cumby, B. L.; Hayes, G. J.; Dickey, M. D.; Justice, R. S.; Tabor, C. E.; Heikenfeld, J. C. Reconfigurable Liquid Metal Circuits by Laplace Pressure Shaping. *Appl. Phys. Lett.* **2012**, *101* (17), 174102.

(21) Neumann, T. V.; Kara, B.; Sargolzaeiaval, Y.; Im, S.; Ma, J.; Yang, J.; Ozturk, M. C.; Dickey, M. D. Aerosol Spray Deposition of Liquid Metal and Elastomer Coatings for Rapid Processing of Stretchable Electronics. *Micromachines* **2021**, *12*, 146.
(22) Lazarus, N.; Bedair, S. S.; Kierzewski, I. M. Ultrafine Pitch Stencil Printing of Liquid Metal Alloys. *ACS Appl. Mater. Interfaces* **2017**, *9* (2), 1178−1182.
(23) Park, T. H.; Kim, J. H.; Seo, S. Facile and Rapid Method for Fabricating Liquid Metal Electrodes with Highly Precise Patterns via One-Step Coating. *Adv. Funct. Mater.* **2020**, *30* (35), No. 2003694.
(24) Ladd, C.; So, J. H.; Muth, J.; Dickey, M. D. 3D Printing of Free Standing Liquid Metal Microstructures. *Adv. Mater.* **2013**, *25* (36), 5081−5085.
(25) Boley, J. W.; White, E. L.; Chiu, G. T. C.; Kramer, R. K. Direct Writing of Gallium-Indium Alloy for Stretchable Electronics. *Adv. Funct Mater.* **2014**, *24* (23), 3501−3507.
(26) Liu, S.; Yuen, M. C.; White, E. L.; Boley, J. W.; Deng, B.; Cheng, G. J.; Kramer-Bottiglio, R. Laser Sintering of Liquid Metal Nanoparticles for Scalable Manufacturing of Soft and Flexible Electronics. *ACS Appl. Mater. Interfaces* **2018**, *10* (33), 28232−28241.
(27) Liu, S.; Reed, S. N.; Higgins, M. J.; Titus, M. S.; Kramer-Bottiglio, R.-B. Oxide Rupture-Induced Conductivity in Liquid Metal Nanoparticles by Laser and Thermal Sintering. *Nanoscale* **2019**, *11*, 17615−17629.
(28) Gozen, B. A.; Tabatabai, A.; Ozdoganlar, O. B.; Majidi, C. High-Density Soft-Matter Electronics with Micron-Scale Line Width. *Adv. Mater.* **2014**, *26* (30), 5211−5216.
(29) Kim, J. H.; Kim, S.; Kim, H.; Wooh, S.; Cho, J.; Dickey, M. D.; So, J. H.; Koo, H. J. Imbibition-Induced Selective Wetting of Liquid Metal. *Nat. Commun.* **2022**, *13* (1), 4763.
(30) Hirsch, A.; Lacour, S. P. A Method to Form Smooth Films of Liquid Metal Supported by Elastomeric Substrate. *Adv. Sci.* **2018**, *5* (10), No. 1800256.
(31) Kramer, R. K.; Boley, J. W.; Stone, H. A.; Weaver, J. C.; Wood, R. J. Effect of Microtextured Surface Topography on the Wetting Behavior of Eutectic Gallium-Indium Alloys. *Langmuir* **2014**, *30* (2), 533−539.
(32) Li, G.; Wu, X.; Lee, D. W. Selectively Plated Stretchable Liquid Metal Wires for Transparent Electronics. *Sens Actuators B Chem.* **2015**, *221*, 1114−1119.
(33) Dejace, L.; Chen, H.; Furfaro, I.; Schiavone, G.; Lacour, S. P. Microscale Liquid Metal Conductors for Stretchable and Transparent Electronics. *Adv. Mater. Technol.* **2021**, *6* (11), No. 2100690.
(34) Kramer, R. K.; Majidi, C.; Wood, R. J. Masked Deposition of Gallium-Indium Alloys for Liquid-Embedded Elastomer Conductors. *Adv. Funct Mater.* **2013**, *23* (42), 5292−5296.
(35) Glenneberg, J.; Andre, F.; Bardenhagen, I.; Langer, F.; Schwenzel, J.; Kun, R. A Concept for Direct Deposition of Thin Film Batteries on Flexible Polymer Substrate. *J. Power Sources* **2016**, *324*, 722−728.
(36) Matsuda, Y.; Kuwata, N.; Okawa, T.; Dorai, A.; Kamishima, O.; Kawamura, J. In Situ Raman Spectroscopy of Li x CoO 2 Cathode in Li/Li 3 PO 4 /LiCoO 2 All-Solid-State Thin-Film Lithium Battery. *Solid State Ion* **2019**, *335*, 7−14.
(37) Trask, J.; Anapolsky, A.; Cardozo, B.; Januar, E.; Kumar, K.; Miller, M.; Brown, R.; Bhardwaj, R. Optimization of 10-Mm, Sputtered, LiCoO2 Cathodes to Enable Higher Energy Density Solid State Batteries. *J. Power Sources* **2017**, *350*, 56−64.
(38) Li, S.; Zhang, H.; Ruan, H.; Cheng, Z.; Yao, Y.; Zhuge, F.; Zhai, T. Programmable Nucleation and Growth of Ultrathin Tellurium Nanowires via a Pulsed Physical Vapor Deposition Design. *Adv. Funct. Mater.* **2023**, *33* (11), No. 2211527.
(39) Ahmad, K. S.; Siraj, H.; Jaffri, S. B.; Alamgir, M. K.; Sohail, M.; Mehmood, R. F.; Rehman, M. U.; Ali, D. Physical Vapor Deposited [Co:Cd-(Dtc)2]/SnO2 Dual Semiconductor Systems: Synthesis, Characterization and Photo-Electrochemistry. *J. Inorg. Organomet. Polym. Mater.* **2021**, *31* (6), 2579−2593.
(40) Chen, C.; Zhang, J.; Du, Y.; Yang, X.; Wang, E. Microfabricated On-Chip Integrated Au-Ag-Au Three-Electrode System for in Situ Mercury Ion Determination. *Analyst* **2010**, *135* (5), 1010−1014.
(41) Ozkucur, N.; Wetzel, C.; Hollstein, F.; Richter, E.; Funk, R. H.; Monsees, T. K. Physical Vapor Deposition of Zirconium or Titanium Thin Films on Flexible Polyurethane Highly Support Adhesion and Physiology of Human Endothelial Cells. *J. Biomed. Mater. Res. A* **2009**, *89* (1), 57−67.
(42) Hirsch, A.; Michaud, H. O.; Gerratt, A. P.; de Mulatier, S.; Lacour, S. P. Intrinsically Stretchable Biphasic (Solid−Liquid) Thin Metal Films. *Adv. Mater.* **2016**, *28* (22), 4507−4512.
(43) Koo, H. J.; So, J. H.; Dickey, M. D.; Velev, O. D. Towards All-Soft Matter Circuits: Prototypes of Quasi-Liquid Devices with Memristor Characteristics. *Adv. Mater.* **2011**, *23* (31), 3559−3564.
(44) Regan, M. J.; Tostmann, H.; Pershan, P. S.; Magnussen, O. M.; Dimasi, E.; Ocko, B. M.; Deutsch, M. X-Ray Study of the Oxidation of Liquid-Gallium Surfaces. *Phys. Rev. B* **1997**, *55* (16), 10786−10790.
(45) Dickey, M. D.; Chiechi, R. C.; Larsen, R. J.; Weiss, E. A.; Weitz, D. A.; Whitesides, G. M. Eutectic Gallium-Indium (EGaIn): A Liquid Metal Alloy for the Formation of Stable Structures in Microchannels at Room Temperature. *Adv. Funct Mater.* **2008**, *18* (7), 1097−1104.
(46) Yu, F.; Xu, J.; Li, H.; Wang, Z.; Sun, L.; Deng, T.; Tao, P.; Liang, Q. Ga-In Liquid Metal Nanoparticles Prepared by Physical Vapor Deposition. *Progress in Natural Science: Materials International* **2018**, *28* (1), 28−33.
(47) Ilyas, N.; Cook, A.; Tabor, C. E. Designing Liquid Metal Interfaces to Enable Next Generation Flexible and Reconfigurable Electronics. *Adv. Mater. Interfaces* **2017**, *4* (15), No. 1700141.
(48) Petrov, I.; Barna, P. B.; Hultman, L.; Greene, J. E. Microstructural Evolution during Film Growth. *Journal of Vacuum Science & Technology A: Vacuum, Surfaces, and Films* **2003**, *21* (5), S117−S128.
(49) Krisnadi, F.; Nguyen, L. L.; Ankit; Ma, J.; Kulkarni, M. R.; Mathews, N.; Dickey, M. D. Directed Assembly of Liquid Metal−Elastomer Conductors for Stretchable and Self-Healing Electronics. *Adv. Mater.* **2020**, *32* (30), No. e2001642.
(50) Lear, T. R.; Hyun, S. H.; Boley, J. W.; White, E. L.; Thompson, D. H.; Kramer, R. K. Liquid Metal Particle Popping: Macroscale to Nanoscale. *Extreme Mech Lett.* **2017**, *13*, 126−134.
(51) Kim, D.; Thissen, P.; Viner, G.; Lee, D. W.; Choi, W.; Chabal, Y. J.; Lee, J. B. Recovery of Nonwetting Characteristics by Surface Modification of Gallium-Based Liquid Metal Droplets Using Hydrochloric Acid Vapor. *ACS Appl. Mater. Interfaces* **2013**, *5* (1), 179−185.
(52) Ki, S.; Shim, J.; Oh, S.; Koh, E.; Seo, D.; Ryu, S.; Kim, J.; Nam, Y. Gallium-Based Liquid Metal Alloy Incorporating Oxide-Free Copper Nanoparticle Clusters for High-Performance Thermal Interface Materials. *Int. J. Heat Mass Transfer* **2021**, *170*, No. 121012.
(53) Lin, W.; Qiu, W.; Tuersun, Y.; Huang, X.; Chu, S. Ultrastrong Spontaneous Surface Wetting of Room Temperature Liquid Metal on Treated Metal Surface. *Adv. Mater. Interfaces* **2021**, *8* (18), No. 2100819.
(54) Ilyas, N.; Butcher, D. P.; Durstock, M. F.; Tabor, C. E. Ion Exchange Membranes as an Interfacial Medium to Facilitate Gallium Liquid Metal Alloy Mobility. *Adv. Mater. Interfaces* **2016**, *3* (9), No. 1500665.
(55) Tang, J.; Zhao, X.; Li, J.; Zhou, Y.; Liu, J. Liquid Metal Phagocytosis: Intermetallic Wetting Induced Particle Internalization. *Adv. Sci.* **2017**, *4* (5), No. 1700024.
(56) Wang, Y.; Gao, Y. N.; Yue, T. N.; Chen, X. D.; Che, R.; Wang, M. Liquid Metal Coated Copper Micro-Particles to Construct Core-Shell Structure and Multiple Heterojunctions for High-Efficiency Microwave Absorption. *J. Colloid Interface Sci.* **2022**, *607*, 210−218.
(57) Handschuh-Wang, S.; Chen, Y.; Zhu, L.; Zhou, X. Analysis and Transformations of Room-Temperature Liquid Metal Interfaces − A Closer Look through Interfacial Tension. *ChemPhysChem* **2018**, *19* (13), 1584−1592.
(58) Deng, Y.; Chen, W.; Li, B.; Wang, C.; Kuang, T.; Li, Y. Physical Vapor Deposition Technology for Coated Cutting Tools: A Review. *Ceram. Int.* **2020**, *46*, 18373−18390.

https://doi.org/10.1021/acsaelm.4c02096
ACS Appl. Electron. Mater. XXXX, XXX, XXX−XXX

(59) Larmagnac, A.; Eggenberger, S.; Janossy, H.; Vörös, J. Stretchable Electronics Based on Ag-PDMS Composites. *Sci. Rep.* **2014**, *4*, 7254.
(60) Lin, R.; Li, Y.; Mao, X.; Zhou, W.; Liu, R. Hybrid 3D Printing All-in-One Heterogenous Rigidity Assemblies for Soft Electronics. *Adv. Mater. Technol.* **2019**, *4* (12), No. 1900614.

https://doi.org/10.1021/acsaelm.4c02096
ACS Appl. Electron. Mater. XXXX, XXX, XXX−XXX